Title
Pulsed Laser Microbeam Cell Lysis: Analysis of Biological Response by Hydrodynamic Modeling and Fluorescence Assays

ISBN
9781557528070

Authors
Hellman, Amy N
Rau, Kaustubh R
Quinto-Su, Pedro A
et al.

Publication Date
2006

DOI
10.1364/bio.2006.tui56

Pulsed Laser Microbeam Cell Lysis: Analysis of Biological Response by Hydrodynamic Modeling and Fluorescence Assays

Amy N. Hellman
Department of Bioengineering, University of California, San Diego, La Jolla, California, 92093
astacy@ucsd.edu

Kaustubh R. Rau
National Centre for Biological Sciences, Tata Institute of Fundamental Research, Bangalore 560 065, INDIA
kaustubh@ncbs.res.in

Pedro A. Quinto-Su and Vasan Venugopalan
Department of Chemical Engineering and Materials Science, University of California, Irvine, 92697
Laser Microbeam and Medical Program, Beckman Laser Institute, Irvine, California 92697
pquintos@uci.edu, vvenugop@uci.edu

Abstract: Time resolved imaging and fluorescent assays were used to examine the biological response of confluent cell cultures to pulsed laser microbeam cell lysis using cavitation bubbles generated by Nd:YAG nanosecond laser pulses at 532 nm.
OCIS codes: (140.3440) Laser-induced breakdown; (140.3540) Lasers, Q-switched; (180.2520) Fluorescence microscopy

1. Introduction

Pulsed laser microbeams offer significant advantages for non-contact manipulation of cells, ranging from subtle perturbations such as cellular microsurgery and transient cell membrane permeabilization to more disruptive processes such as cell lysis. The versatility of laser microbeams has led researchers to explore uses in biotechnology, such as for the manipulation of cells for cell analytics. Despite the innovative utilization of laser microbeams in biology, there have been relatively few studies on the basic mechanisms of laser-induced cell injury due to the challenges posed by the small spatial and rapid time scales over which these processes occur. A better understanding of the interaction of pulsed laser microbeams with cells is necessary for progression of laser microbeams from research tools into useful applications.

Time-resolved imaging provides a method to capture dynamic phenomena on nanosecond timescales with micrometer precision. In addition to acquiring visual data, image analysis provides quantitative data that can be used to develop models for cellular response to laser generated forces. Our lab has developed a time-resolved imaging system capable of visualizing events on the sub-nanosecond to microsecond timescale, with micrometer spatial and nanosecond temporal resolutions to capture the dynamics of the cell injury process [1]. This system is currently integrated within a laser microbeam/microscope platform that delivers nanosecond laser pulses to adherent cells cultures. The dynamics of laser-induced cell lysis caused by 6 ns pulses have been studied and we have developed physical models of cell lysis based on experimental data.

2. Results

Figure 1 depicts a series of images taken at different time points during the cell lysis process at a pulse energy of 30 μJ in a Petri-dish containing a monolayer of cultured PtK_2 cells. The plasma formation and subsequent dynamics along with the development of the cell lysis process could be captured in great detail. Plasma initiation, growth, and decay were complete within 25-30 ns after the arrival of the laser pulse with the maximum plasma diameter being 20 μm. Vaporization of cells due to the high temperature plasma could not be visualized due to the plasma luminescence. Close examination of Figure 1a reveals the formulation of a pressure shock wave resulting from the rapid expansion of the plasma whose propagation could then be followed until it passed outside of view (Fig. 1a-d). Estimates of pressure amplitudes indicated that they can approach 500 MPa close to the irradiation site (Rau, Guerra et al. 2004). However, the pressure wave passage did not cause any visible disruption within the cell monolayer; an indication of its minimal impact on cell injury.

The plasma expansion resulted in cooling and ion-recombination, thereby leading to the formation of a cavitation bubble within 25 ns following the laser pulse. Figures 1c-g reveal that cavitation bubble expansion is the

primary mechanism of cell lysis and several interesting features of this process can be seen in these images. At early times (35-250 ns) during the expansion of the cavitation bubble, the outer portions of the bubble appear dark due to the oblique angle of incidence of the illumination pulse on the bubble surface that prevented its transillumination. Even at these time points cell injury was clearly visible within the central region of the bubble (Fig. 1d-e). Thus the onset of cellular injury is on the order of tens of nanoseconds. Cell lysis progressed as the bubble expansion continued thereby expanding the zone of cellular injury. This zone of injury reached its final size within 300 ns for irradiation with 30 μJ pulse energy. Beyond this time point, further bubble expansion did not result in additional cellular injury. Instead, further bubble growth incorporated the cells without lysing them (Fig. 1g). Another interesting feature was the cellular deformation produced by the bubble expansion, evident both outside and inside the bubble (Fig. 1f-g). Remarkably, these cells appeared to withstand this severe deformation without disruption. After reaching its maximum size, the subsequent bubble collapse phase as seen in Figure 1h was rapid (1-2 μs). The bubble was seen to break up upon collapse without any coherent structures such as jet formation (Fig. 1i). The bubble collapse did not produce further cellular injury but did clear the cellular debris present in the lysis zone. As a result, at the end of the process, a well defined area around the irradiation site was cleared of cells and cellular debris (Fig. 1j) that we define as the zone of cellular injury.

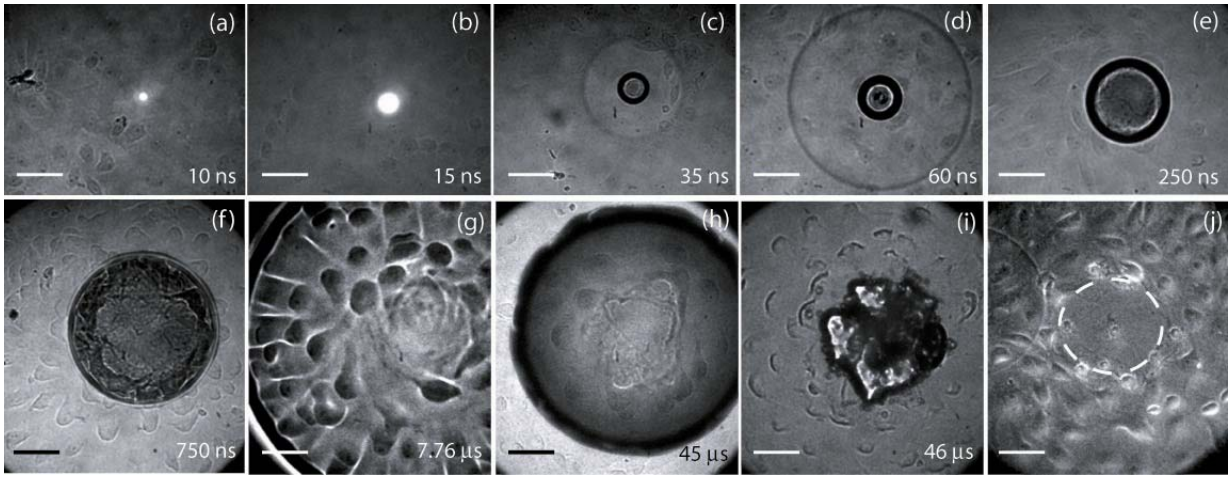

Fig. 1: Time-resolved image series of cell lysis produced by a 30 μJ pulse showing cavitation bubble dynamics and development of the injury process. Image times are as marked. Fig. 6j is a phase contrast image and shows the cell sample post irradiation, with the dotted circle marking the lysis zone. Scale bar = 50 μm.

Quantitative image analysis of the time-resolved images allowed assessment of the effects of the cavitation bubble expansion and collapse to determine the dynamic shear stresses inflicted on the cells. The time-resolved images were analyzed to determine the maximum bubble radius and collapse time. The temporal evolution of the bubble size was plotted and the bubble velocity was determined from this data. Hydrodynamic modeling was then performed in order to relate cellular injury characteristics to hydrodynamics (i.e. fluid velocities and shear stresses). To estimate the shear stresses produced and thereby correlate them to observed effects, we modeled the flow field experienced by adherent cells. The boundary layer width and wall shear stress were calculated based on convolving the time evolution of the external fluid velocity with the solution to Stokes' first problem for 1-D planar impulsive flow. These modeling results showed that regardless of pulse energy, cells at the edge of the injury zone that experienced a maximum shear stress less than 180-220 kPa remained adherent, most likely because the time of interaction is less than 1 ms. The maximum shear stresses for pulse energies of 7-30 μJ ranged from 180-220 kPa at the rim of the lysis region.

To relate the physical effects of the shear stresses caused by the cavitation bubble expansion to the biological response of the adherent cells surrounding the zone of lysis, we performed a variety of fluorescent assays. These assays examined cell viability, the extent of membrane permeabilization, and the integrity of the cell cytoskeleton and focal adhesion contacts after exposure to 6 ns laser pulses. The extent of damage was confirmed by performing a standard live-dead fluorescence assay with calcein AM and propidium iodide staining of the cell cultures after irradiation. Cell membrane permeabilization was assessed by examining uptake of fluorescein isothiocyanate (FITC) conjugated dextran (4 kDa) that was added to the extracellular medium prior to cell lysis. Figure 2 shows the results of cell viability and membrane permeabilization assays. We observed that only cells on the edge of the lysis zone

were dead as determined by PI uptake (Fig. 2a). Cells elsewhere in the field of view remained viable as shown by calcein AM uptake (Fig. 2b), even after experiencing significant deformation due to the outward fluid flow (cf. Fig. 1). The cell deformation did cause membrane permeabilization as shown by the uptake of dextran from the extracellular medium (Fig. 2d). This indicated that induced strain was large enough to produce membrane pores that allowed exogenous molecules to enter the cells. However, these pores were small enough such that they could repair over time, allowing the cell to survive.

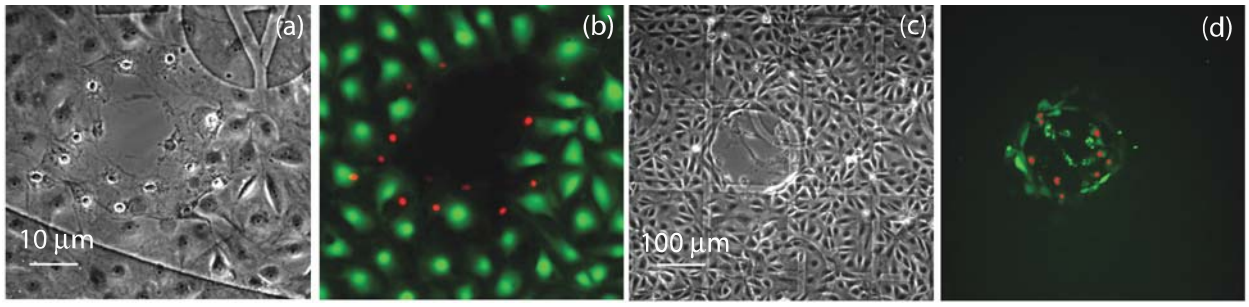

Fig. 2: Cellular response to focused laser pulses assessed by fluorescence assays. (a) and (c) are phase contrast images of two different areas imaged after exposure to one laser pulse with their corresponding fluorescence images shown in (b) and (d). In (b) results of a viability assay show live cells stained with calcein AM (green) and dead cells stained with propidiumk iodide (red). In (d) membrane permeabilization in cells surrounding the lysis site is exhibited by uptake of fluorescently labeled dextran (green), with dead cells being stained with PI (red).

To determine changes in cell architecture and morphology, we examined both control and laser-irradiated cell samples after co-staining for cytoskeletal actin (Fig. 3). Focal adhesion contacts were also observed by immunofluorescent labeling of vinculin at cell-cell and cell-substrate contacts. We observed that except for cells adjacent to the lysis zone there was little or no disruption or rearrangement of fibular actin in cells exposed to cavitation bubbles. Similarly, we did not observe a decrease in vinculin at focal adhesion sites or beyond the periphery of the damaged zone, indicating that there was no significant disruption of cell-cell or cell-substrate contacts in these cells.

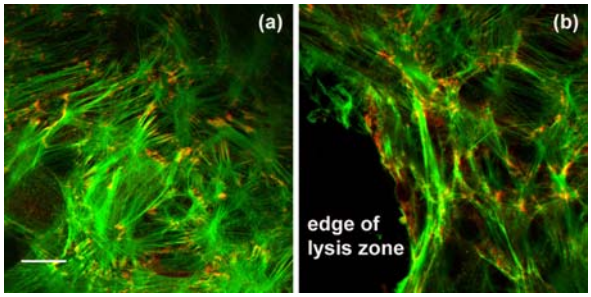

Fig. 3: Cytoskeleton and focal adhesion contacts: (a) control site with no laser irradiation, (b) on edge of damage zone after laser irradiation. Actin network is shown in green, vinculin is shown in red. Scale bar = 10 µm.

3. Conclusion

Time-resolved image analysis determined that the shear stress produced by the bubble expansion was the primary contributor to cell lysis at separation distance of 10 µm above the cell monolayer. The hydrodynamic analysis and fluorescence assays discussed show that adherent cells on the border of the lysis region can withstand shear stresses in the 180-220 kPa range without damage or detachment while maximum shear stresses are in the range of 6-28 kPa at 100 µm from the irradiation site while maintaining viability. Permeabilization studies revealed that cells were transiently permeabilized up to 50 µm around the lysis zone, indicating that shear stresses were sufficient to produce a transient, but repairable, disruption in the plasma cell membrane. Minimal cytoskeletal changes were seen in cells outside the lysis zone and focal adhesions remained strong.

4. References

[1] Rau, K., A. Guerra, et al.. "Investigation of laser-induced cell lysis using time-resolved imaging." APPLIED PHYSICS LETTERS **84**(15): 2940-2942(2004).